High-temperature cyclic oxidation of Pt-rich γ-γ' bond-coatings. Part II: Effect of Pt and Al on TBC system lifetime

Pauline Audigié[a,*], Aurélie Rouaix-Vande Put[a], André Malié[b], Carole Thouron[a], Daniel Monceau[a]

[a] CIRIMAT, University of Toulouse, ENSIACET, 4 Allée Emile Monso, BP 44362, 31030, Toulouse Cedex 4, France
[b] SAFRAN Aircraft Engines, 99 rue Maryse Bastié, BP 129, 86101, Châtellerault Cedex, France

ARTICLE INFO

ABSTRACT

Three kinds of Pt-rich γ-γ' bond-coating were processed with different contents in Pt and Al. The cyclic oxidation tests performed at 1100 °C on TBC systems showed the superiority of the Pt-rich γ-γ' coatings when compared with the β-(Ni,Pt)Al reference system. TBCs with a Pt-only bond-coating provided the highest performance. Whatever the bond-coating, the failure occurred at the TGO/bond-coating interface which appeared to be the weak point of these γ-γ' bond-coating based systems. Al addition during bond-coating fabrication did not improve the durability. A decrease of 2 μm of electroplated Pt thickness led to a higher performance than the reference systems.

1. Introduction

Thermal Barrier Coating (TBC) failure characterized by macroscopic spallation of the ceramic yttria partially stabilized zirconia (YSZ) can be caused by thermal and/or mechanical stresses [1–3], sulphur segregation [4–7], rumpling [8–12] or even void formation after very-long term exposure at high temperature [13]. For this study, the high temperature oxidation behaviour of systems without top coat was firstly investigated while in a second part, the complete TBC systems were studied. In part I of this study [14], emphasis was placed upon the cyclic oxidation kinetics of superalloy / coating systems after very long-term exposure at 1100 °C. Pt-rich γ-γ' bond-coatings on AM1 doped in hafnium showed superior oxidation resistance than the reference system with a β-(Ni,Pt)Al coating. Among the Pt-rich γ-γ' tested compositions, the best thermal cycling resistance was observed for Pt + Al γ-γ' coatings prepared from a platinum electroplating and a "short-term" aluminizing step, when compared with Pt-only γ-γ' coatings after 6000 cycles of 1 h at 1100 °C. Aluminium addition during fabrication was thus leading to an improvement of the cyclic oxidation performance of superalloy/coating systems.

In order to corroborate such results to the industrial application, cyclic oxidation performance of complete TBC systems with Pt-only γ-γ' and Pt + Al γ-γ' bond-coatings was investigated. Cyclic oxidation tests at 1100 °C were performed to determine the spallation kinetics and the degradation mechanism of TBC systems with a Pt-rich γ-γ' bond-coating. The effect of coating composition was also studied from five compositions of Pt-rich γ-γ' bond-coatings.

2. Experimental

AM1 first-generation single-crystal superalloy with a low sulphur content (< 0.4 ppm) and a hafnium doping of about 500 ppmw was used as substrate. The base composition of the AM1 alloy was Ni-12Al-9Cr-7Co-2Ti-3Ta-2W-1Mo (at.%), with 0.12S-570Hf-25Zr-23C (ppmw). Superalloys coupons (2 mm thick, 24 mm of diameter) were grit-blasted with α-Al$_2$O$_3$ particles before deposition. Three main kinds of bond-coatings were fabricated and were named P for Pt-only γ-γ', PA for Pt + Al γ-γ' and B for β-(Ni,Pt)Al as described in the Table 1. Pt-only γ-γ' coatings were prepared by electroplating 5 ± 2 μm of Pt on AM1 superalloy followed by an annealing for 1 h in vacuum at 1100 °C. Four variants of the Pt + Al γ-γ' coatings were prepared from either 5 ± 2 μm or 7 ± 2 μm of electroplated platinum, a heat treatment for 1 h under vacuum at 1100 °C and a "short-term" aluminizing. This latter corresponds to an interrupted high temperature low activity vapor phase aluminizing (APVS®) treatment. This latter is composed of four steps as cited in [15]:

- Formation of a gaseous phase in the cement allowing aluminium transport,
- Transport of this gaseous phase to the sample surface,
- Chemical reduction on the sample surface with aluminium extraction from the gaseous phase,
- Solid diffusion of deposited aluminium in the sample.

---

* Corresponding author.
 E-mail addresses: audigiep@inta.es (P. Audigié), Carole.thouron@ensiacet.fr (C. Thouron).

P. Audigié et al.

Table 1
Sample designation and TBC fabrication conditions. In sample ID, P = Pt, PA = Pt + Al and B = β. The asterisk * indicates the sample characterized in the as-prepared condition.

Sample ID	Target coating	Fabrication Conditions				Equivalent Pt (μm)	Equivalent Al (μm)	Run
		Pt	Heat Treatment	Al	Top coat			
TBC-P1 *	Pt-only	5 μm	1h, 1100 °C under vacuum	–	EBPVD	4.8	–	2
TBC-P2	γ-γ'					4.7	–	
TBC-P3	5/0					4.9	–	
TBC-P4						4.9	–	
TBC-PA1 *	Pt + Al	5 μm		# 1		5.7	1.5	1
	γ-γ'							
	5/2							
TBC-PA2						5.6	1.7	
TBC-PA3						5.3	0.8	
TBC-PA4 *	Pt + Al	5 μm		# 2		5.3	2.1	1
	γ-γ'							
	5/5							
TBC-PA5						5.3	2.1	
TBC-PA6						5.5	1.5	
TBC-PA7 *	Pt + Al	5 μm		# 3		5.0	7.0	2
	γ-γ'							
	5/5							
TBC-PA8						4.6	5.6	
TBC-PA9						4.7	6.4	
TBC-PA10						4.8	5.2	
TBC-PA11 *	Pt + Al	7 μm		# 1		6.9	1.7	1
	γ-γ'							
	7/2							
TBC-PA12						6.8	1.7	
TBC-PA13						7.1	2.4	
TBC-PA14						7.3	2.4	
TBC-PA15 *	Pt + Al	7 μm		# 2		7.2	2.9	1
	γ-γ'							
	7/5							
TBC-PA16						7.4	2.2	
TBC-PA17						7.0	3.1	
TBC-PA18						6.9	2.2	
TBC-B1	β-(Ni,Pt)Al	7 μm		APVS		7.0		1
TBC-B2						7.0		
TBC-B3 *	β-(Ni,Pt)Al					6.7	~ 22	
TBC-B4						6.6		2
TBC-B5						6.8		

The usual aluminizing temperature and time of the APVS® are respectively 1100 °C ± 50 °C and between 4 h and 6 h [15]. In this study, the aluminizing treatment depended on two main factors: the activator quantity which plays a role in the formation of the gaseous phase and the dwell time at high temperature. These parameters were adjusted in order to deposit the equivalent of a layer of either 5 μm or 2 μm of aluminium. A dwell time of 1 h was applied in both cases. Half quantity of activator than usual APVS® was used to deposit 5 μm of Al while no activator was used to deposit 2 μm. For a detailed description of the "short-term" aluminizing, the reader is referred to [16]. The Pt layer thickness and equivalent Al thickness were calculated from the mass gain after electroplating and aluminizing step by considering that each deposit was fully dense. Coatings were named with their platinum/aluminium target equivalent thicknesses. Coatings were hence referred to as the 5/2, 5/5, 7/2 and 7/5 compositions. But the actual Pt and Al equivalent thicknesses were different from the targets and are given in Table 1.

For comparison purpose, conventional TBC systems with β-(Ni,Pt)Al coatings were fabricated from a 7 ± 2 μm thick platinum layer by electroplating, a diffusion heat treatment of 1 h under vacuum at 1100 °C and a conventional vapor phase aluminizing (APVS). For all systems, a ~150 μm thick 8 wt.% yttria stabilized zirconia top coat was deposited by electron-beam physical vapor deposition (EBPVD) during two different runs. During the run 1, top coat was deposited on both sides of the coupons while only one side was coated during the run 2. This deposition detail did not affect the results of the study because the

observed side for samples from both runs was the chamfered one.

Sample designation and fabrication conditions are detailed in Table 1. One sample of each system was characterized after fabrication; those samples were defined as reference and are indicated with an asterisk in Table 1.

Cyclic oxidation tests with cycles composed of a 1 h dwell at 1100 °C and an air forced 15 min cooling down to room temperature were performed on all systems. Samples were removed periodically from the cyclic oxidation rig to be photographed in order to follow spallation kinetics during thermal cycling. Pictures were used to determine the YSZ unspalled area fraction by image analysis. The lifetime criteria was arbitrarily defined as 75% of unspalled area fraction. Thus, samples were removed from the cyclic oxidation tests and examined post-mortem. Cross-sections of TBC systems were characterized by scanning electron microscopy (SEM LEO 435 V P) and energy dispersive spectroscopy (IMIX EDS) from real standards in order to determine which led to failure, i.e. to top coat spallation. Both techniques were also used to characterize the reference samples. As a precision, coating chemical compositions were measured by EDS and correspond to the concentrations averaged on all the coating thickness. Rectangular zones of 215 μm wide and the coating thickness high were drawn to measure the composition. Therefore the height of the analyzed window was adjusted depending on the observed microstructure. It is thus noteworthy that the precision of the measure is theoretically lower when a two-phased volume is analyzed when compared with a single-phase volume but this difference was not quantified.
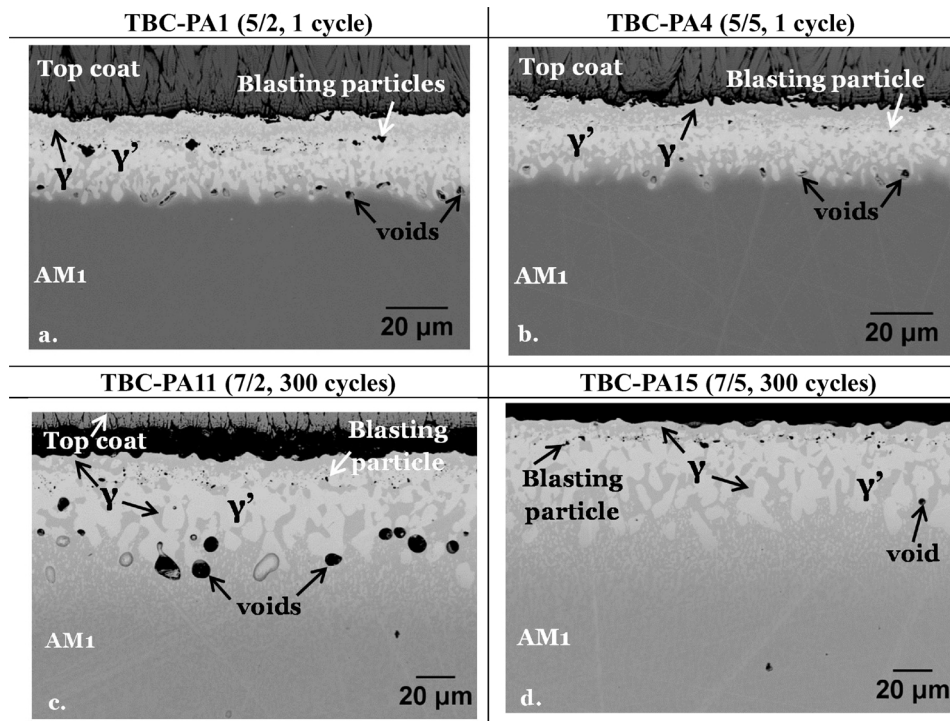
Fig. 1. Backscattered electron images of metallographic cross-sections of the Pt + Al γ-γ' bond-coatings from the run 1: (a, b) TBC-PA1 and TBC-PA4 in the as-annealed condition, (c, d) TBC-PA11 and TBC-PA15 after 300 cycles at 1100 °C.

3. Results and discussion

3.1. As-fabricated coatings

The TBC-PA1 and TBC-PA4 reference systems were characterized after fabrication whereas the TBC-PA11 and TBC-PA15 systems were analyzed after 300 cycles at 1100 °C. Fig. 1 corresponds to the back-scattered electron images of the cross-sections of these fourth reference systems and shows the typical microstructure of Pt-rich γ-γ' bond-coatings. Residual alumina particles from the grit-blasting marked the original substrate surface. Above the grit-blasting particles, the coating mainly consisted of a mixture of the γ-Ni and γ'-Ni₃Al phases enriched in Pt. Below the original surface, the coating consisted of large grains of γ' precipitated in a γ-matrix. By considering the lower limit of the large inward growing Pt-rich γ' grains, the thicknesses of the PA1 and PA4 coatings after fabrication were 26.0 ± 2.0 µm and 23.6 ± 2.0 µm, respectively (to compare, the β-(Ni,Pt)Al coating TBC-B3 had an average thickness of 62.6 ± 3.0 µm). Chemical compositions of each bond-coating were determined by EDS as an average on all the coating thickness and are reported in Table 2. Whatever the coating

composition, the platinum and aluminium concentrations were lower than the expected target. Aluminium concentration was comprised between 12 and 17 at.% while the platinum one was 19 at.% at the most after fabrication. In addition, voids were observed at the bond-coating / superalloy interface in all the systems. Neither secondary reaction zones (SRZ) nor topologically-close packed (TCP) phases were observed.

After fabrication, the EBPVD top coat had a good adhesion to the bond-coating due to the formation of a thin layer of Al₂O₃ during TBC processing.

Additional systems were fabricated in a second processing run in order to obtain coatings with larger platinum and aluminium con-centrations for Pt + Al γ-γ' systems. These systems were referenced with the "run 2″ tag. These corresponded to the Pt-only γ-γ' coatings (TBC-P1 to P4), some 5/5 Pt + Al coatings (TBC-PA7 to PA10) and some β-(Ni,Pt)Al coatings (TBC-B3 to B5), the latter being considered as the industrial reference system. The microstructure of these three sys-tems after fabrication was similar to the ones of systems without top coat (Fig. 2) [14]. The average chemical compositions of the γ-γ' zones for the Pt-only (TBC-P1), Pt + Al γ-γ' (TBC-PA7) coatings and of the β layer for the β-(Ni,Pt)Al coating (TBC-B3) are reported in the Table 2.

Table 2
Chemical compositions in at.% of all the reference bond-coatings, in the as-annealed condition for the TBC-P1, TBC-PA1, TBC-PA4, TBC-PA7 and TBC-B3 systems and after 300 cycles at 1100 °C for the TBC-PA11 and TBC-PA15 systems.

| Sample ID	Target coating	Ni	Al	Pt	Cr	Co	Ti	Ta	W	Mo	Hf
TBC-P1	Pt-only γ-γ' (run 2)	49.6	14.1	18.1	6.1	4.5	1.7	2.8	1.6	1.4	–
TBC-PA1	Pt + Al γ-γ' 5/2	47.2	17.0	18.6	5.3	4.1	1.7	3.1	1.5	1.5	–
TBC-PA4	Pt + Al γ-γ' 5/5	50.4	12.7	16.5	7.4	5.2	1.7	2.8	1.5	1.9	–
TBC-PA7	Pt + Al γ-γ' 5/5 (run 2)	47.5	17.5	18.8	4.2	4.0	2.0	3.7	0.8	1.0	0.4
TBC-PA11	Pt + Al γ-γ' 7/2	56.4	16.1	9.0	5.7	4.6	2.3	3.4	1.5	1.2	–
TBC-PA15	Pt + Al γ-γ' 7/5	59.1	14.6	7.6	5.3	4.6	2.4	3.8	1.2	1.3	–
TBC-B3	β-(Ni,Pt)Al (run 2)	37.7	44.0	11.0	3.1	2.9	0.3	0.2	0.1	0.4	0.2

P. Audigié et al.
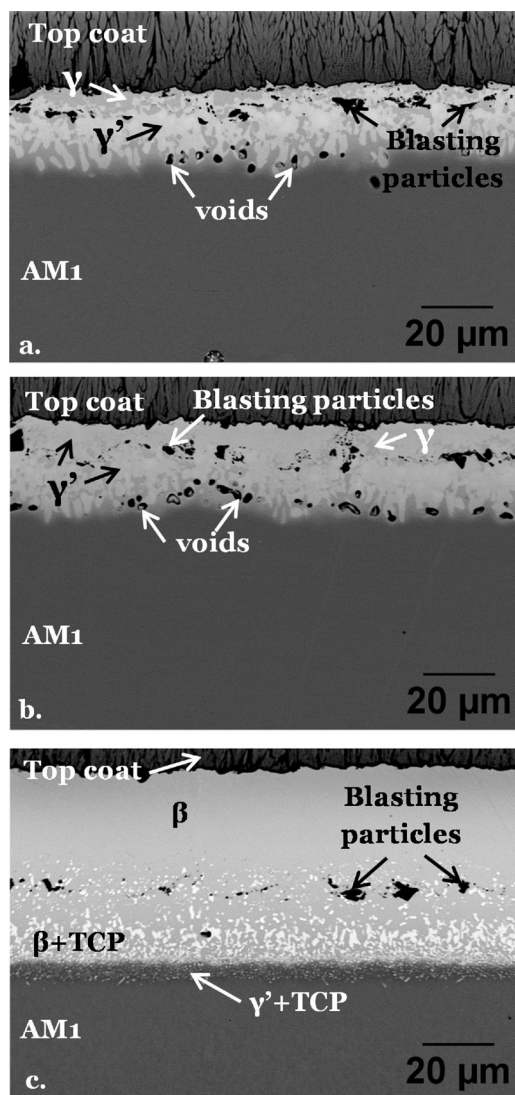
Fig. 2. Backscattered electron images of the cross-section of the reference bond-coatings from the run 2: (a) TBC-P1, (b) TBC-PA7 and (c) TBC-B3 samples.

Platinum contents of the Pt-rich γ-γ' coatings were close to the ones of systems from the run 1 (16.5 to 19 at%). The aluminium concentration varied between 12.7 at% and 17.7 at% and was poorly correlated with the amount of Al diffused in the coatings during the process (Table 1). We observed that the aluminium concentration of the TBC-PA1 system in the as-fabrication conditions was higher than the one of the TBC-PA4 system although this latter theoretically contained less aluminium according to the aluminium equivalent thickness calculations. Indeed, a 1.5 μm aluminium equivalent thickness and a 13.9 at.% of aluminium were estimated for the TBC-PA1 system while a 2.1 μm thickness and 10.9 at.% were obtained for the TBC-PA4. This difference can be explained on one hand by the thermodynamic effect of platinum on the aluminium activity [17], promoting the very fast uphill aluminium diffusion from the fabrication step [18].

Cr and Ti concentrations were similar in all γ-γ' coatings, except for the Pt-only γ-γ' coating which had a slightly higher Cr concentration (6.1 at%) than others.

It appears that the different γ-γ' coatings are differentiated by their quantity of diffused Al, and somehow by the quantity of Pt electro-deposited (Table 1), but this is not clearly visible in the average surface composition of the fabricated coatings.

3.2. Spallation kinetics

Fig. 3 exhibits the progression of the top coat spallation for one sample of each system during thermal cycling at 1100 °C. Most of the samples showed localized spallation close to the edges due to a geometrical effect ("the edge effect"). Then spallation progressed towards the disc center, which is clearly visible for TBC-PA10 and TBC-PA18 samples.

As demonstrated by the macroscopic pictures, the lifetime of the systems was increased of about 200 cycles when the platinum equivalent thickness increased from 5.3 μm to 6.9 μm whereas the aluminium level remained close. For a similar platinum content, the TBC system lifetime was extended of more than 400 cycles when the aluminium addition increased from 2.1 μm to 5.2 μm.

In order to better identify the platinum and aluminium effects described above, the YSZ unspalled area fraction was plotted versus the number of cycles at 1100 °C (Figs. 4 and 5). The maximum number of cycles undergone by each system was also indicated on the figures.

Despite identical conditions for thermal cycling, reference systems with a β-(Ni,Pt)Al coating showed a lifetime dispersion from 600 to 1350 cycles. The whole top coat was spalled for two samples of the run 1 after 1000 cycles while two others arose from the run 2 reached the lifetime criteria after about 1300 cycles. Local analyses were conducted by Raman spectroscopy on the YSZ spalled flakes. The tetragonal and monoclinic phases were detected on the YSZ of the run 1 whereas only tetragonal phase was identified on the YSZ of the run 2. Thus, the lifetime dispersion was attributed to the presence of the monoclinic phase, which is known to be detrimental for thermal cycling resistance [19]. For this reason, results from run 1 and run 2 were plotted in separate figures.

Looking at systems from the run 1, the 5/2 systems showed the poorest performance with time to failure of 395 cycles (TBC-PA3) and 565 cycles (TBC-PA2). Then one sample of each bond-coating composition (TBC-PA6, TBC-PA12, TBC-PA16) was removed from the cyclic oxidation tests in order to compare the system microstructures after the same number of cycles (565 cycles). Other samples were tested until the lifetime criterion was reached. Two behaviours of the TBC-PA bond-coating systems stood out by comparison with the reference system. On one hand, for lower initial platinum content than in the reference system and for the lowest initial aluminium content, TBC-PA systems were less performing than the reference systems, as demonstrated by the TBC-PA2 and TBC-PA3 samples containing less than 2 μm equivalent thickness of aluminium. On the other hand, for a similar or even lower initial platinum equivalent thickness (5 μm instead of 7 ± 2 μm) but with a sufficient aluminium addition, TBC cyclic oxidation resistance greatly increased and was superior to the one of the conventional systems. Indeed, most of the samples had preserved more than 95% of the zirconia top coat after more than 1000 cycles at 1100 °C. The TBC-PA18 sample provided the longest life span of 1340 cycles of 1 h at 1100 °C. Considering that AM1 contains a great quantity of titanium, this was clearly promising since the time to failure of TBC systems with the same sample geometry, an EBPVD top coat and either a β-(Ni,Pt)Al or a MCrAlY coating was almost never exceeded 1000 cycles at 1100 °C [20–23].

Platinum and aluminium additions during fabrication seem to play a key role in the ceramic spallation and influence the TBC lifetime. Globally, the larger the additions were, the longer lifetime was for the γ-γ' bond coatings.

Considering systems from the run 2, TBCs lifetimes increased and even reached time to failure of 1250 and 1365 cycles at 1100 °C for the TBC-B reference systems containing a β-(Ni,Pt)Al coating. All the TBC-P systems with a Pt-rich γ-γ' bond-coating exhibited a better oxidation resistance than the reference systems, except for the TBC-PA8 sample which suffered from desktop spalling (DTS) [24]. The longest lifetimes were provided by the TBC-P systems with a Pt-only γ-γ' bond-coating with time to failure from 1455 to 2300 cycles, which is an exceptionally
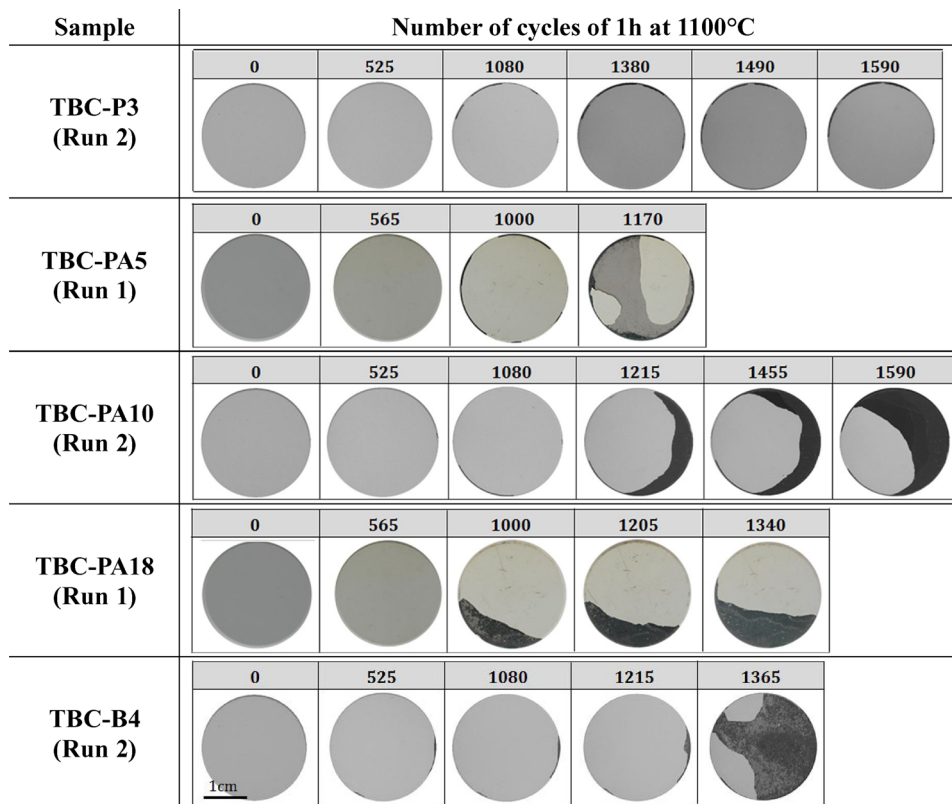
Fig. 3. Progression of the top coat spallation for one sample of each system during thermal cycling at 1100 °C.
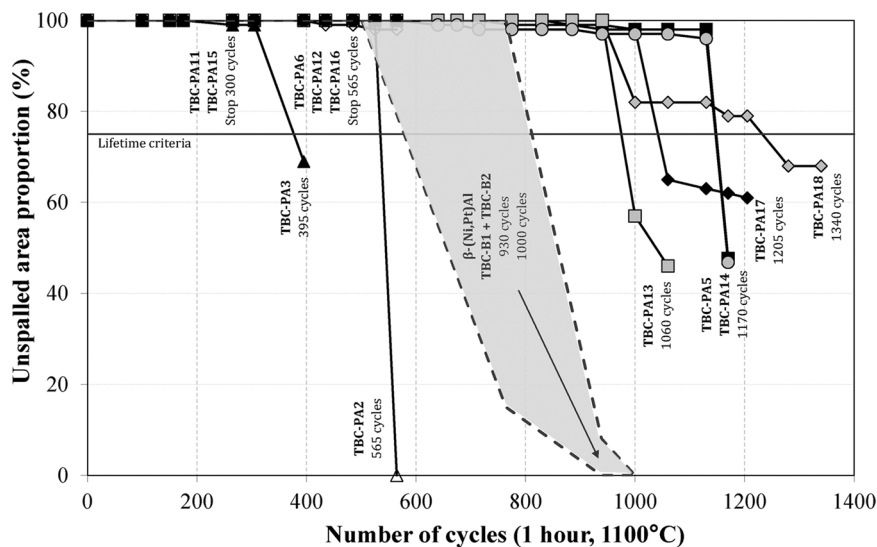

Fig. 4. Spallation kinetics of systems from run 1 after thermal cycling at 1100 °C.

long life for an EBPVD YSZ on AM1 superalloy.

Keeping in mind that all the Pt-rich γ-γ' coatings from the run 2 were fabricated with 5 μm of electroplated platinum instead of 7 ± 2 μm in the β-(Ni,Pt)Al coatings, a reduction of 2 μm of electro-plated platinum led to a similar or even higher performance than re-ference systems. However, the beneficial effect of aluminium evidenced with systems from the run 1 was not observed for systems from run 2. This result was thus surprising because the Pt-only γ-γ' coatings in systems without top coat have previously shown that they were an "amplifier" of the detrimental effect of the titanium and tantalum by supporting the formation of the TiTaO$_4$ oxide and the oxide spallation [14]. But, this last observation was done after very-long term exposure

(more than 3000 cycles). Consequently, according to the present study, aluminium addition during bond-coating fabrication does not enhance TBC performance. Conversely, this work shows that excellent perfor-mances of resistance to thermal cycling of TBC systems are obtained with about 5 μm of electroplated Pt, whatever the Al addition, and that the best behaviour is even obtained without Al addition.

The excellent cyclic oxidation resistance of the TBC-P systems could be explained by the presence of voids at the interdiffusion zone / substrate interface. Voids observed after fabrication may prevent the inward platinum diffusion and/or the outward nickel diffusion, this being responsible for the delay of the YSZ spallation. TBC systems can have an excellent cyclic oxidation resistance but a poor mechanical
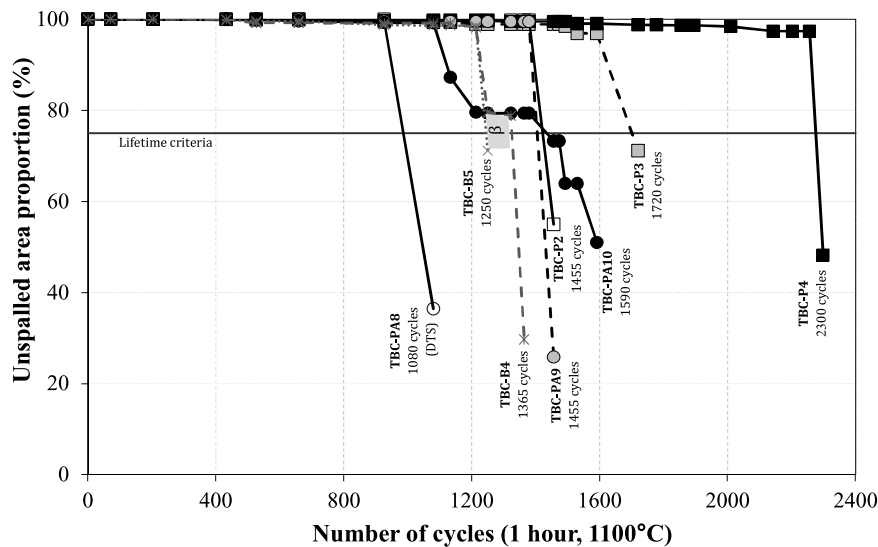
Fig. 5. Spallation kinetics of systems from run 2 after thermal cycling at 1100 °C.

behaviour under external stresses. The effect of porosity on the mechanical behaviour of the coating under stress needs to be assessed.

Another interpretation of the excellent behaviour of the Pt-only γ-γ' bond-coating could also be a larger creep resistance due to a higher Pt concentration, and therefore lower rumpling kinetics. At the moment, data are lacking to discuss further on this point.

3.3. Microstructure after thermal cycling

Comparison of the microstructures of TBC systems after cyclic oxidation did not reveal any major difference between all kinds of coatings. Fig. 6 shows the end-of-life microstructure of the TBC-PA5 sample after 1170 cycles at 1100 °C. Similarly to all the systems, the PA bond-coating had a duplex structure with a continuous single-phase γ layer below the TGO and a two-phase γ-γ' layer with large Pt-rich γ' grains. The thicknesses of these two zones were different between all systems, those depended on the time to failure but also on the initial platinum and aluminium additions. As an example, the γ layer of the TBC-PA5 sample was 9.8 ± 2.0 μm thick after 1170 cycles while the γ-γ' layer was 42.8 ± 7.2 μm thick. Besides, voids were also observed at the bond-coating / superalloy interface but in a smaller proportion when compared with the as-received state.

Chemical compositions of the best performing sample of each system were determined by EDS after thermal cycling (Table 3). As an example, the γ-γ' layer of the TBC-PA5 system maintained aluminium level (11.7 at.%) close to the one found in the as-deposited state (12.7
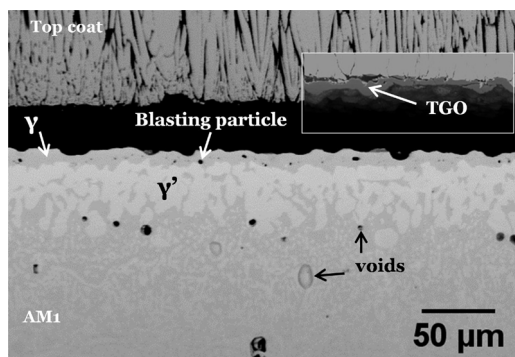
at.%) while the platinum content decreased from 16.5 at.% to 4.6 at.% in 1170 cycles. After the same duration, the γ layer of this system contained 7.7 at.% of aluminium and 4.0 at.% of platinum. High concentrations of chromium (16.1 at.%) and cobalt (8.3 at.%) were also detected in the subsurface layer.

Failure occurred at the oxide / bond-coating interface in all cases. Only Al_2O_3 could be detected in the TGO; precisely alumina was observed at the base of the YSZ columns with a thickness comprised between 5 and 7 μm at the failure for all the systems. Moreover, no rumpling, no TCP phases and no SRZ were observed whatever the composition of the Pt-rich γ-γ' coatings. These results demonstrated that the oxidation performance of TBC systems with a Pt-rich γ-γ' coating is mainly predominated by the TGO / γ interface. Improving chemical bounds between these two layers is necessary to enhance oxidation performance.

3.4. Influence of the initial chemical composition

To easily compare the oxidation performance and to better visualize the influence of the bond-coating composition, a Pt-Al performance map was plotted (Fig. 7) where the lifetime was represented versus the platinum and aluminium equivalent thicknesses (see Table 1). In systems fabricated by spark plasma sintering, Selezneff et al. [22] previously reported that it exists a critical aluminium level necessary to sustain the growth of the protective alumina scale and to avoid top coat spallation. However, according to the present study, this schema was not confirmed since systems without aluminium addition had the best oxidation behaviour. Nevertheless, the Pt-Al map illustrates that a reduction of 2 μm of platinum led to excellent oxidation performance.

Then, in order to correlate the microstructure, the chemical composition and the lifetime of TBCs, SEM observations coupled with EDS analyses were conducted on all the systems from the run 1. Concentrations of platinum and aluminium after fabrication and thermal cycling were reported in Fig. 8. The SEM image in the upper right of the figure indicates the zone where concentrations have been measured. Fig. 8 shows that aluminium and platinum concentrations decreased in the coating to finally tend towards the aluminium concentration in the AM1 (11.6 at.%). This progression was more or less rapid depending on the initial platinum and aluminium contents. For instance, the aluminium concentration decreased from 20 at.% to 13 at. % in 700 cycles for the TBC-PA15 system while it decreased from 14 at. % to 12.5 at.% in 530 cycles for the TBC-PA1 system. Platinum concentrations also decreased more or less quickly during thermal cycling

Fig. 6. End-of-life microstructure of the TBC-PA5 sampleafter 1170 cycles at 1100 °C (SEM-BSE).

Table 3
Chemical compositions in at.% of the most resistant sample of each system at the failure time.

Sample ID	Target Coating	Time at failure (cycles)	Zone	Ni	Al	Pt	Cr	Co	Ti	Ta	W	Mo	Hf
TBC-P4	Pt-only	2300	γ	59.3	6.3	2.8	15.0	8.9	1.1	1.9	2.7	2.1	0.1
	(run 2)		γ-γ'	61.0	10.8	3.3	9.5	6.9	1.8	3.1	2.1	1.5	0.1
TBC-PA2	Pt + Al	565	γ	56.7	7.7	4.5	15.8	8.1	1.0	1.5	2.4	2.5	–
	γ-γ'		γ-γ'	58.1	12.5	5.1	10.4	6.3	1.6	2.5	1.7	1.8	–
	5/2												
TBC-PA5	Pt + Al	1170	γ	56.3	7.7	4.0	16.1	8.3	1.0	1.6	2.4	2.6	–
	γ-γ'		γ-γ'	59.1	11.7	4.6	10.3	6.4	1.7	2.7	1.8	1.8	–
	5/5												
TBC-PA10	Pt + Al	1590	γ	57.9	7.4	3.6	14.8	8.4	1.3	1.7	2.4	2.4	0.1
	γ-γ'		γ-γ'	58.7	11.9	4.2	10.0	6.8	1.9	2.7	2.0	1.7	0.1
	5/5												
	(run 2)												
TBC-PA14	Pt + Al	1170	γ	55.3	7.4	4.9	16.4	8.2	0.9	1.7	2.6	2.5	–
	γ-γ'		γ-γ'	58.4	14.0	6.4	7.1	5.1	2.1	3.5	1.9	1.4	–
	7/2												
TBC-PA18	Pt + Al	1340	γ	57.0	7.1	3.8	16.5	8.6	0.9	1.5	2.3	2.5	–
	γ-γ'		γ-γ'	59.4	12.2	3.9	9.9	6.5	1.5	2.8	2.2	1.7	–
	7/5												
TBC-B4	β-(Ni,Pt)Al	1365	γ'	57.7	21.4	5.9	5.2	5.0	1.4	1.7	0.8	0.7	0.3
	(run 2)		β	45.7	34.0	8.1	6.8	3.8	0.6	0.3	0.1	0.5	0.1
			β + TCP	58.3	19.6	4.6	5.2	5.3	1.5	2.5	1.4	1.2	0.3

to finally be close to 4 at.% for all systems when failure occurred. Globally, the failures occurred for all systems for about 4–6 at% of Pt and 11.7–13.5 at.% of Al, i.e. only slightly higher of similar than the AM1 Al concentration. This value is much higher than the critical Al content (5.9 at.%) observed at breakaway for coated AM1 without a top coat (first part of this study [14]).

These promising results, in terms of thermal cycling resistance were obtained on a first generation nickel-based superalloy doped in hafnium but containing a large amount of titanium. As the Pt-rich γ-γ' bond-coatings are highly sensitive to the superalloy composition and titanium is known to be detrimental for resistance to cyclic oxidation, the cyclic oxidation resistance of these TBCs could be even improved by using a Ti-free substrate.

4. Conclusion

The objective of this work was to study the effect of the bond-coating composition on the cyclic oxidation durability of TBC systems with a Pt-rich γ-γ' bond-coating. Three kind of bond-coatings were processed depending on their platinum and aluminium additions.

The oxidation tests performed on complete TBC systems pointed out the superiority of the Pt-rich γ-γ' coatings when compared with the reference β-(Ni,Pt)Al system. Except for two systems which contained monoclinic phase in the zirconia top coat, all systems had lifetimes superior to 1000 cycles of 1 h at 1100 °C which was very promising when compared with literature data for the same superalloy and top coat. In particular, TBCs with a Pt-only γ-γ' bond-coating provided the highest performance with an exceptional lifetime of up to 2300 cycles
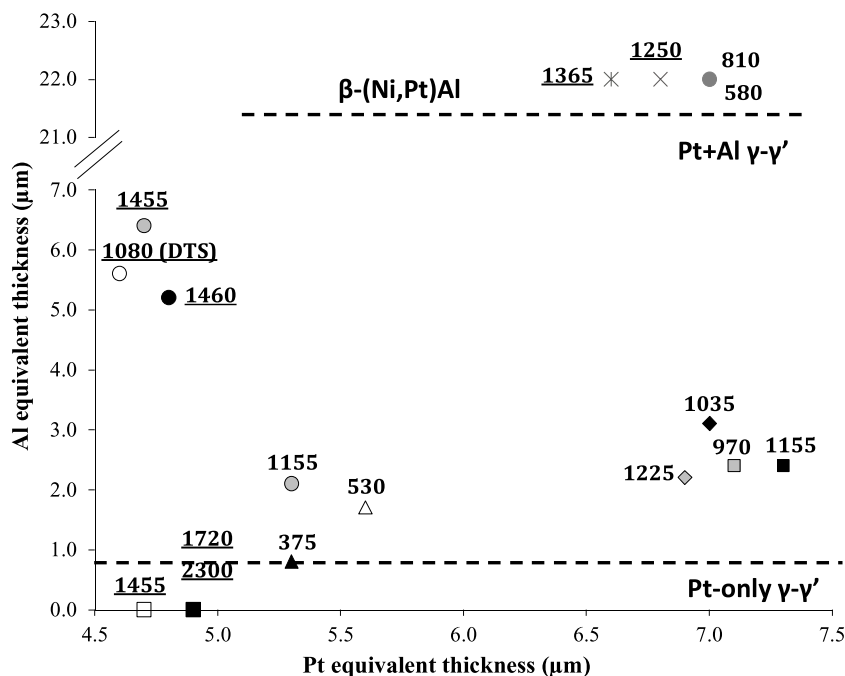

Fig. 7. Life span of all the systems depending on their Pt and Al initial additions (Pt and Al equivalent thicknesses). DTS = Desktop Spalling. Results from Run 2 are underlined.
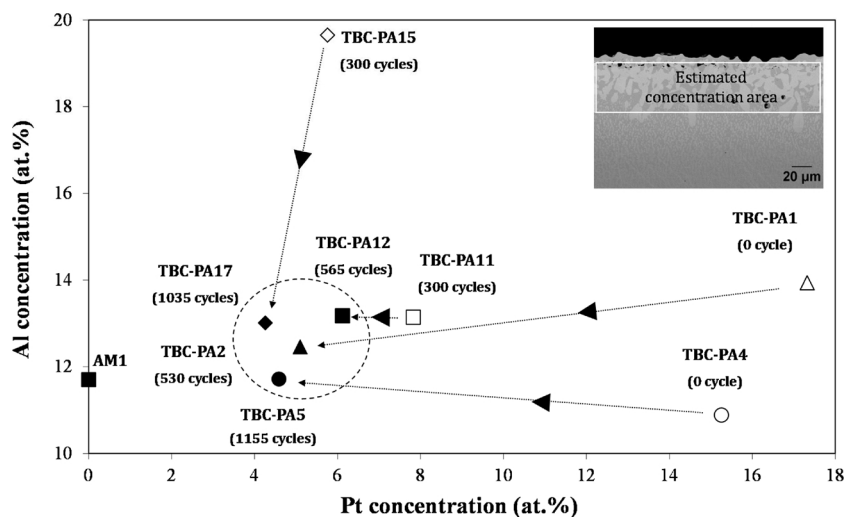
Fig. 8. Evolution with time of the platinum and aluminium concentrations in the remaining part of the coatings (samples from Run 1).

at 1100 °C. Contrary to the results obtained for the same systems without top coat, aluminium addition during the bond-coating fabrication did not improve the durability of the TBCs with a Pt-rich γ-γ' coating. This was explained by the fact that TBC systems failed much earlier than the breakaway observed on coated superalloy without top coat. The Al addition during manufacturing is beneficial for a very long life (more than 5 or 10 thousands hours at 1100 °C), because of the consumption of Al by oxidation, but the Al addition is not necessary and apparently even detrimental for a TBC life of 2000 h. TBC systems fail earlier than breakaway of the bond-coating (i.e. chemical failure) because of the effect of mechanical stresses during thermal cycling. The level of Al in the bond-coating at failure of the TBC does not seem to be critical, but the Pt concentration could be critical. Pt level in the coating and just below the TGO plays a role on the adhesion of the TGO and certainly a role on the mechanical properties of the bond-coating. Further work is needed to confirm this assumption.

For the studied systems of the present work, it was shown that a reduction of 2 μm of electroplated platinum led to higher performance than the reference systems after thermal cycling. Therefore, the reduction of the platinum layer thickness together with the suppression of the aluminizing step allow improved performances at a reduced manufacturing cost.

Whatever the bond-coating, the failure occurred at the TGO / bond-coating interface where the subsurface γ' layer transformed into γ during exposure at high temperature. Improving the adhesion between the oxide and the γ layer acts for the new challenge to enhance oxidation performance of TBCs with a Pt-rich γ-γ' coating.

Acknowledgements

References

[1] D.M. Lipkin, D.R. Clarke, M. Hollatz, M. Bobeth, W. Pompe, Stress development in alumina scales formes upon oxidation of (111) NiAl single crystals, Corros. Sci. 39 (2) (1997) 231–242.

[2] V.K. Tolpygo, D.R. Clarke, Microstructural study of the theta-alpha transformation in alumina scales formed on nickel-aluminides, Mater. High Temp. 17 (1) (2000) 59–70.

[3] D.M. Lipkin, C. D.R, Measurement of the stress in oxide scales formed by oxidation of alumina-forming alloys, Oxid. Met. 45 (3-4) (1996) 267–280.

[4] A.W. Funkenbusch, J.G. Smeggil, N.S. Bornstein, Reactive Element-Sulfur Interaction and oxide scale adherence, Metal. Trans. A 16A (1985) 1164–1166.

[5] P.Y. Hou, J. Stringer, Oxide Scale adhesion and impurity segregation at the scale/metal interface, Oxid. Met. 38 (5/6) (1992) 323–345.

[6] J.A. Haynes, M.J. Lance, B.A. Pint, I.G. Wright, Characterization of commercial EB-PVD TBC systems with CVD (Ni,Pt)Al bond coatings, Surf. Coat. Technol. 146–147 (2001) 140–146.

[7] Y. Cadoret, M.-P. Bacos, P. Josso, V. Maurice, P. Marcus, S. Zanna, Study of the sulfur segregation on Pt-modified Nickel Aluminides and its influence on the TBC spallation mechanism, Mater. Sci. Forum (2004) p.

[8] Y. Zhang, J.A. Haynes, B.A. Pint, I.G. Wright, W.Y. Lee, Martensitic transformation in CVD NiAl and (Ni,Pt)Al bond coatings, Surf. Coat. Technol. 163 (2003) 19–24.

[9] V.K. Tolpygo, D.R. Clarke, On the rumpling mechanism in nickel-aluminide coatings. Part II: characterization of surface undulations and bond coat swelling, Acta Mater. 52 (2004) 5129–5141.

[10] D.S. Balint, T. Xu, J.W. Hutchinson, A.G. Evans, Influence of bond coat thickness on the cyclic rumpling of thermally grown oxides, Acta Mater. 54 (7) (2006) 1815–1820.

[11] V.K. Tolpygo, D.R. Clarke, Temperature and cycle-time dependence of rumpling in platinum-modified diffusion aluminide coatings, Scr. Mater. 57 (7) (2007) 563–566.

[12] V.K. Tolpygo, D.R. Clarke, Rumpling of CVD (Ni,Pt)Al Diffusion Coatings under Intermediate Temperature Cycling, Surf. Coat. Technol. (2009) 3278–3285.

[13] A.G. Evans, D.R. Clarke, C.G. Levi, The influence of oxides on the performance of advanced gas turbines, J. Eur. Ceram. Soc. 28 (2008) 1405–1419.

[14] P. Audigié, A. Rouaix-Vande Put, A. Malié, D. Monceau, High-temperature cyclic oxidation behavior of Pt-rich γ-γ' bond-coatings. Part I: oxidation kinetics of coated AM1 systems after very long-term exposure at 1100°C, Corros. Sci. 144 (2018) 127–135.

[15] J. Benoist, K.F. Badawi, A. Malié, C. Ramade, Microstructure of Pt-modified aluminide coatings on Ni-based superalloys, Surf. Coat. Technol. 182 (2004) 14–23.

[16] P. Audigié, Modélisation de l'interdiffusion et du comportement en oxydation cyclique de superalliages monocristallins à base de nickel revêtus d'une sous-couche γ-γ' riche en platine. Extension aux systèmes barrière thermique., PhD Thesis, Institut National Polytechnique de Toulouse, 2015, http://www.theses.fr/2015INPT0054.

[17] B. Gleeson, W. Wang, S. Hayashi, D. Sordelet, Effects of Platinum on the Interdiffusion and oxidation Behavior of Ni-Al-Based Alloys, Mater. Sci. Forum 461-464 (2004) 213–222.

[18] P. Audigié, A. Rouaix-Vande Put, A. Malié, P. Bilhé, S. Hamadi, D. Monceau, Observation and modeling of alpha-NiPtAl and Kirkendall void formations during interdiffusion of a Pt coating with a gamma-(Ni-13Al) alloy at high temperature, Surf. Coat. Technol. 260 (2014) 9–16.

[19] J.H. Wood, E.H. Goldman, Protective coatings, in: N.S.S, C.T. Sims, W.C. Hagel (Eds.), Superalloys II, Wiley, New York, 1987, pp. 359–384.

[20] A. Vande Put, D. Oquab, A. Raffaitin, D. Monceau, Effect of Pt addition on the cyclic oxidation resistance of NiCoCrAlYTa base TBC systems, EUROCORR, (2009) Nice.

[21] R.T. Wu, X. Wang, A. Atkinson, On the interfacial degradation mechanisms of thermal barrier coating systems: effects of bond coat composition, Acta Mater. 58 (17) (2010) 5578–5585.

[22] S. Selezneff, M. Boidot, J. Hugot, D. Oquab, C. Estournès, D. Monceau, Thermal cycling behavior of EBPVD TBC systems deposited on doped Pt-rich gamma-gamma prime bond coatings made by Spark Plasma Sintering (SPS), Surf. Coat. Technol. 206 (2011) 1558–1565.

[23] J.L. Smialek, Compiled furnace cyclic lives of EB-PVD thermal barrier coatings, Surf. Coat. Technol. 276 (2015) 31–38.

[24] J.L. Smialek, Moisture-Induced Delayed Alumina Scale Spallation on a Ni(Pt)Al Coating, (2009) NASA/TM-2009-215664.